

Ferromagnetically ordered metal in the single-band Hubbard model

Akihisa Koga,¹ Yusuke Kamogawa,¹ and Joji Nasu²

¹*Department of Physics,
Tokyo Institute of Technology,
Meguro,
Tokyo 152-8551,
Japan^{a)}*

²*Department of Physics,
Yokohama National University,
79-5 Tokiwadai,
Hodogaya,
Yokohama 240-8501,
Japan*

(Dated: 12 December 2019)

Abstract. We study a ferromagnetic instability in a single-band Hubbard model on the hypercubic lattice away from half filling. Using dynamical mean-field theory with the continuous-time quantum Monte Carlo simulations based on the segment algorithm, we calculate the magnetic susceptibility in the weak and strong coupling regions systematically. We then find how ferromagnetic fluctuations are enhanced when the interaction strength and density of holes are varied. The efficiency of the double flip updates in the Monte Carlo simulations is also addressed.

Ferromagnetism in a metallic state has attracted much interest since rare-earth-based permanent magnets has recently been synthesized such as Nd-Fe-B. In contrast to the multiorbital systems such as manganites, the ferromagnetic instability in single-band models is less understood. When the static mean-field approximation is applied to the model, one meets the Stoner criterion, where the Coulomb interaction yields a ferromagnetic instability in the system with a large density of states (DOS) at the Fermi level. The criterion is qualitatively correct when the interaction strength is small. In fact, the ferromagnetically ordered states is realized in the single band systems with flat bands [1, 2, 3, 4, 5, 6, 7] and asymmetric DOS [8, 9, 10, 11]. On the other hand, the Stoner theory is inapplicable in the strong coupling regime. In this limit, itinerant nature of one hole in the Hubbard model on a lattice with a closed-loop structure leads to a fully polarized ferromagnetically ordered ground state, which is so-called Nagaoka ferromagnetism [12]. However, still controversial how this ordered state relates to the system with the finite hole density. What is the most important in this strong-coupling region is that large Coulomb interactions and low energy itinerant properties of electron are necessary to deal with precisely in an equal footing. Therefore, it is desired to access the strongly correlated region by means of reliable techniques.

In our previous paper [13], we have examined the ferromagnetic instability in the single-band Hubbard model by means of dynamical mean-field (DMFT) theory and the continuous-time quantum Monte Carlo (CTQMC) simulations. Then, we have clarified that the ferromagnetically ordered state is realized in the hypercubic lattice, but it does not in the Bethe lattice. Unlike the weak coupling regime, our previous results indicates that the noninteracting density of states with a slower decay in the high-energy region plays an important role in realizing the ferromagnetically ordered state at low temperatures. It is also instructive to clarify how magnetic fluctuations are enhanced in the paramagnetic metallic region. To this end, we study, in the paper, the magnetic instability in the single-band Hubbard model on the hypercubic lattice.

We consider the doped single-band Hubbard model, which should be given as,

$$H = -t \sum_{(i,j),\sigma} (c_{i\sigma}^\dagger c_{j\sigma} + \text{h.c.}) + U \sum_i n_{i\uparrow} n_{i\downarrow} - \sum_{i\sigma} (\mu + \frac{h}{2}\sigma) n_{i\sigma}, \quad (1)$$

where $c_{i\sigma}$ ($c_{i\sigma}^\dagger$) is the annihilation (creation) operator of an electron with spin σ ($=\uparrow, \downarrow$) at the i th site and $n_{i\sigma} = c_{i\sigma}^\dagger c_{i\sigma}$. t is the hopping integral, U is the on-site Coulomb interaction, μ is the chemical potential, and h is the external magnetic field.

^{a)}Corresponding author: A. Koga koga@phys.titech.ac.jp

To clarify magnetic properties in the Hubbard model on the hypercubic lattice, we make use of DMFT [14, 15, 16, 17]. In DMFT, the lattice model is mapped to a single impurity model connected dynamically to a “heat bath”. The electron Green’s function is self-consistently obtained via this impurity problem. The treatment is exact in the infinite dimensions and DMFT has successfully explained magnetic properties in single-band [13, 18, 19, 20, 21] and multi-orbital models [22, 23, 24, 25, 26, 27, 28].

In DMFT, the selfenergy is represented to be site-diagonal $\Sigma_\sigma(k, z) = \Sigma_\sigma(z)$ and the lattice Green’s function is given as

$$G_\sigma(k, z)^{-1} = G_{0\sigma}(k, z)^{-1} - \Sigma_\sigma(z), \quad (2)$$

where $G_{0\sigma}(k, z)^{-1} = z + \mu + \frac{h}{2}\sigma - \varepsilon_k$, $\varepsilon_k (= -2t \sum_i^d \cos k_i)$ is the dispersion relation, and d is the dimension. The local Green’s function is then obtained as

$$G_{loc,\sigma}(z) = \int dk G_\sigma(k, z) = \int dx \frac{\rho_0(x)}{z + \mu + \frac{h}{2}\sigma - x - \Sigma_\sigma(i\omega_n)}, \quad (3)$$

where we have introduced the non-interacting DOS for the hypercubic lattice

$$\rho_0(x) = \int dk \delta(x - \varepsilon_k) = \frac{1}{\sqrt{\pi D}} \exp\left[-\left(\frac{x}{D}\right)^2\right], \quad (4)$$

where $D (= 2\sqrt{dt})$ is the normalized energy scale characteristic of the tightbinding model on the hypercubic lattice ($d \rightarrow \infty$). The Dyson equation in the effective impurity model is given as,

$$\mathcal{G}_\sigma(z)^{-1} = G_{imp,\sigma}(z)^{-1} + \Sigma_{imp,\sigma}(z), \quad (5)$$

where $\mathcal{G}(z)$ is the effective bath. We then obtain the selfenergy and Green function, solving the effective impurity model. We iterate the procedure so as to satisfy the selfconsistency conditions $G_\sigma(z) = G_{imp,\sigma}(z)$ and $\Sigma_\sigma(z) = \Sigma_{imp,\sigma}(z)$ until the desired numerical accuracy is achieved.

In this manuscript, we discuss magnetic properties in the doped single-band Hubbard model, by calculating the uniform magnetization and magnetic susceptibility. These are defined as,

$$m = \frac{1}{2} (\langle n_\uparrow \rangle - \langle n_\downarrow \rangle), \quad \chi = \lim_{\Delta h \rightarrow 0} \frac{\Delta m}{\Delta h}, \quad (6)$$

where $n_\sigma = \sum_i n_{i\sigma}/N$ and N is the number of sites. In our study, we numerically evaluate the magnetic susceptibility by the magnetization induced by a tiny external magnetic field; Δm is given by the difference between m for $h = \Delta h$ and that for $h = 0$. Here, we study the nature of the ferromagnetic metallic state in the single-band Hubbard model. To this end, we do not consider the antiferromagnetically ordered state and phase separation, which might be realized near half filling [19, 29], where $n = \sum_\sigma \langle n_\sigma \rangle$. This enables us to clarify the essence of the ferromagnetic instability in the large- U region.

In our calculations, we employ the strong-coupling version of the CTQMC method [30, 31] based on the segment algorithm, which is one of the powerful methods to solve the effective impurity model. In the method, Monte Carlo samplings are performed by local updates such as insertion (removal) of a segment or empty space between segments (antisegment). However, the acceptance probability for the updates p_S is exponentially suppressed while increasing the interaction strength U , typically around $n \sim 1$. Therefore, it is difficult to evaluate the Green’s function in the reasonable computational cost. Now, we consider additional updates, where the configuration for both spins in a certain interval is simultaneously changed. This double flip update enables us to perform the CTQMC method in the strong-coupling region efficiently [13, 25, 26, 32]. Figure 1 shows the acceptance ratios p_S and p_D for the standard and double flip updates in the case with $U/D = 50$ and 1000 at a fixed temperature $T/D = 0.01$. It is found that around $n \sim 1$, the double flip update processes are almost accepted ($p_D \sim 1$), while the standard updates little occur ($p_S \ll 1$). Therefore, we can say that the double flip updates are necessary to evaluate magnetic quantities accurately. On the other hand, away from half filling, the system becomes metallic, where p_S rapidly increases and p_D decreases. When $U/D = 1000$, the uniform magnetization appears when $0.85 < n < 0.99$, as shown in Fig. 1(b). In the case, the update process for the spin inversion is hard to be accepted, namely p_D is suppressed.

Using the above update processes in the Monte Carlo simulations, we study magnetic properties in the single band Hubbard model on the hypercubic lattice. Figure 2(a) shows the electron density dependence of the susceptibility in the weak coupling region at $T/D = 0.01$. When the system is noninteracting ($U = 0$), the susceptibility is proportional to the noninteracting density of states at Fermi level. Therefore, the susceptibility takes a maximum at $n = 1$. The

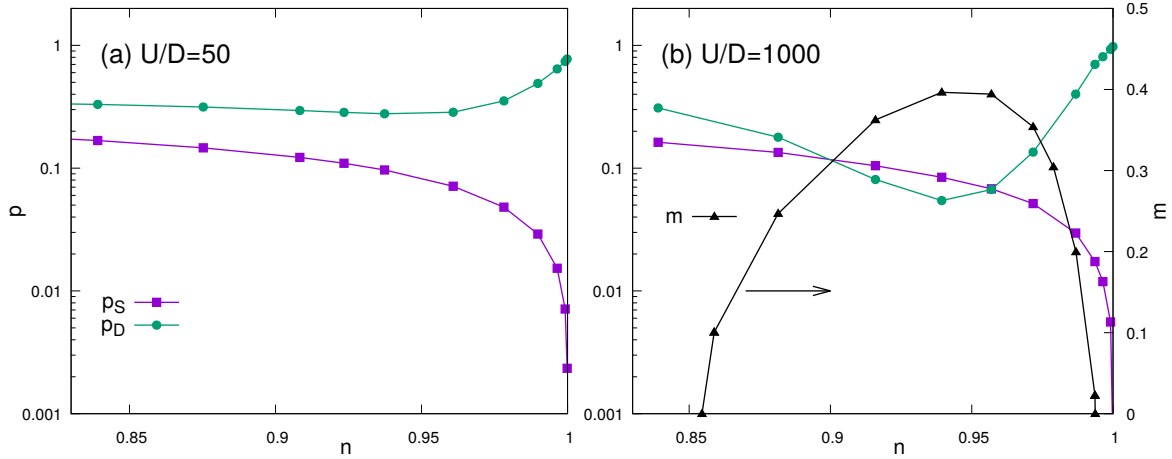


FIGURE 1. The acceptance ratios for simple and double flip updates as a function of the electron density n in the system with $U/D = 50$ (a) and $U/D = 1000$ (b) when $T/D = 0.01$. Triangles in (b) represent the spontaneous magnetization.

introduction of the Coulomb interaction enhances magnetic fluctuations, typically, around $n \sim 1$, as seen in Fig. 2(a). We find that in the case with $U/D = 5$, the magnetic susceptibility takes a maximum away from $n = 1$. This should indicate the ferromagnetic instability away from half filling. To clarify how the ferromagnetic instability appears in the strong coupling region, we show in Fig. 2(b) the contour plot of the magnetic susceptibility in the model at $T/D = 0.01$. When the interaction strength increases, nonmonotonic behavior in the susceptibility appears as a

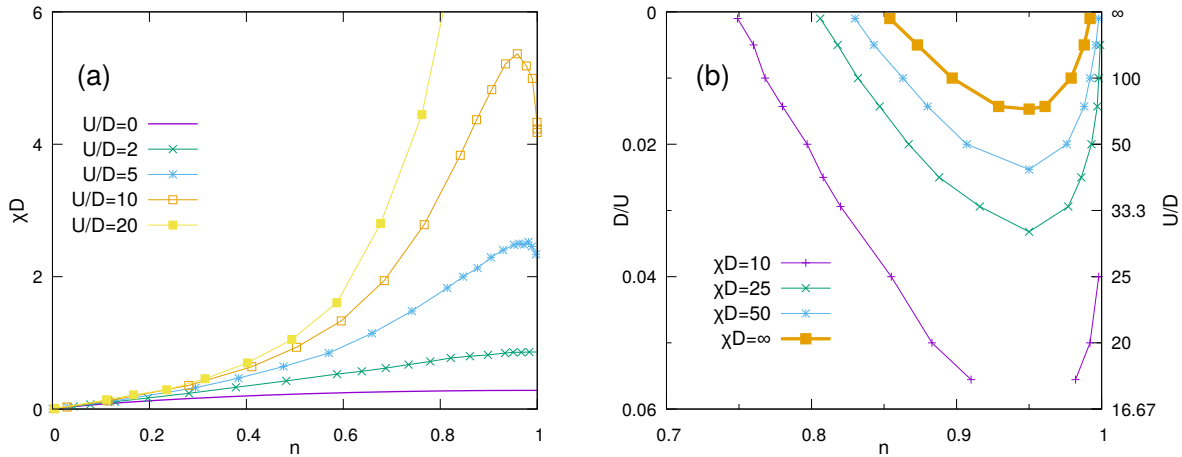


FIGURE 2. (a) Magnetic susceptibility as a function of electron filling in the system with $U/D = 0, 2, 5, 10,$ and 20 at $T/D = 0.01$. (b) Contour plot of the magnetic susceptibility in the single-band Hubbard model when $T/D = 0.01$. The bold line represents the phase boundary between the paramagnetic and ferromagnetic phases, which is determined by the divergence of the susceptibility.

function of the filling n . When the Coulomb interaction is fixed as a certain value ($U/D \lesssim 70$), the peak structure in the susceptibility is always located around $n \sim 0.95$, in contrast to the weak coupling region. Further increase of the interaction strength U drives the system to the ferromagnetically ordered state, where the second-order phase transition occurs with a divergence of the magnetic susceptibility. This is in contrast to the single-band Hubbard model on the Bethe lattice. In the case, the maximum in the susceptibility is always located at $n = 1$ [13], which suggests that the ferromagnetic instability is hindered by the antiferromagnetic order. On the other hand, in the case of the hypercubic lattice, the maximum location away from $n = 1$ indicates the appearance of the ferromagnetic order in the system. It is an interesting problem to clarify whether or not the ferromagnetic instability is indeed present in the single-band Hubbard model in the finite dimensions, which is now under consideration.

We have studied a ferromagnetic instability in a single-band Hubbard model on the hypercubic lattice away from half filling, combining dynamical mean-field theory with the continuous-time quantum Monte Carlo simulations. By calculating the magnetic susceptibility systematically, we have clarified how ferromagnetic fluctuations are enhanced in the paramagnetic metallic state.

ACKNOWLEDGMENTS

Parts of the numerical calculations were performed in the supercomputing systems in ISSP, the University of Tokyo. This work was supported by Grant-in-Aid for Scientific Research from JSPS, KAKENHI Grant Nos. JP19H05821, JP18K04678, JP17K05536 (A.K.), JP16H02206, JP18H04223, JP19K03742, and by JST PREST (JPMJPR19L5) (J.N.). The simulations have been performed using some of the ALPS libraries [33].

REFERENCES

1. A. Mielke, *J. Phys. A* **24**, 3311 (1991).
2. A. Mielke, *J. Phys. A* **25**, 4335 (1992).
3. A. Mielke, *Phys. Lett. A* **174**, 443–448 (1993).
4. H. Tasaki, *Phys. Rev. Lett.* **69**, 1608 (1992).
5. K. Kusakabe and H. Aoki, *Phys. Rev. Lett.* **72**, 144 (1994).
6. S. Miyahara, K. Kubo, H. Ono, Y. Shimomura, and N. Furukawa, *J. Phys. Soc. Jpn.* **74**, 1918–1921 (2005).
7. K. Noda, A. Koga, N. Kawakami, and T. Pruschke, *Phys. Rev. A* **80**, 063622 (2009).
8. J. Kanamori, *Prog. Theor. Phys.* **30**, 275–289 (1963).
9. M. Ulmke, *Eur. Phys. J. B* **1**, 301 (1998).
10. J. Wahle, N. Blümer, J. Schlipf, K. Held, and D. Vollhardt, *Phys. Rev. B* **58**, 12749–12757 (1998).
11. M. Balzer and M. Potthoff, *Phys. Rev. B* **82**, 174441 (2010).
12. Y. Nagaoka, *Phys. Rev.* **147**, 392–405 (1966).
13. Y. Kamogawa, J. Nasu, and A. Koga, *Phys. Rev. B* **99**, 235107 (2019).
14. W. Metzner and D. Vollhardt, *Phys. Rev. Lett.* **62**, 324–327 (1989).
15. E. Müller-Hartmann, *Z. Phys. B* **74**, 507–512 (1989).
16. A. Georges, G. Kotliar, W. Krauth, and M. J. Rozenberg, *Rev. Mod. Phys.* **68**, 13–125 (1996).
17. T. Pruschke, M. Jarrell, and J. Freericks, *Adv. Phys.* **44**, 187–210 (1995).
18. R. Chitra and G. Kotliar, *Phys. Rev. Lett.* **83**, 2386 (1999).
19. R. Zitzler, T. Pruschke, and R. Bulla, *Eur. Phys. J. B* **27**, 473 (2002).
20. R. Zitzler, N.-H. Tong, T. Pruschke, and R. Bulla, *Phys. Rev. Lett.* **93**, 016406 (2004).
21. A. Koga, T. Saitou, and A. Yamamoto, *J. Phys. Soc. Jpn.* **82**, 024401 (2013).
22. T. Momoi and K. Kubo, *Phys. Rev. B* **58**, R567–R570 (1998).
23. S.-y. Miyatake, K. Inaba, and S.-i. Suga, *Phys. Rev. A* **81**, 021603 (2010).
24. H. Yanatori and A. Koga, *J. Phys. Soc. Jpn.* **85**, 014002 (2015).
25. H. Yanatori and A. Koga, *Physical Review B* **94**, 041110 (2016).
26. A. Koga and H. Yanatori, *J. Phys. Soc. Jpn.* **86**, 034702 (2017).
27. K. Ishigaki, J. Nasu, and A. Koga, *J. Phys. Soc. Jpn.* **88**, 024702 (2019).
28. K. Ishigaki, J. Nasu, A. Koga, S. Hoshino, and P. Werner, *Phys. Rev. B* **99**, 085131 (2019).
29. T. Obermeier, T. Pruschke, and J. Keller, *Phys. Rev. B* **56**, R8479–R8482 (1997).
30. P. Werner, A. Comanac, L. de’ Medici, M. Troyer, and A. J. Millis, *Phys. Rev. Lett.* **97**, 076405 (2006).
31. E. Gull, A. J. Millis, A. I. Lichtenstein, A. N. Rubtsov, M. Troyer, and P. Werner, *Rev. Mod. Phys.* **83**, 349–404 (2011).
32. A. Koga and P. Werner, *Phys. Rev. A* **84**, 023638 (2011).
33. B. Bauer, L. D. Carr, H. G. Evertz, A. Feiguin, J. Freire, S. Fuchs, L. Gamper, J. Gukelberger, E. Gull, S. Guertler, A. Hehn, R. Igarashi, S. V. Isakov, D. Koop, P. N. Ma, P. Mates, H. Matsuo, O. Parcollet, G. P. owski, J. D. Picon, L. Pollet, E. Santos, V. W. Scarola, U. Schollwöck, C. Silva, B. Surer, S. Todo, S. Trebst, M. Troyer, M. L. Wall, P. Werner, and S. Wessel, *J. Stat. Mech.* **2011**, P05001 (2011).
34. T. Moriya and A. Kawabata, *J. Phys. Soc. Jpn.* **34**, 639–651 (1973).
35. T. Moriya and Y. Takahashi, *J. Phys. Soc. Jpn.* **45**, 397 (1978).
36. K. K. Murata and S. Doniach, *Phys. Rev. Lett.* **29**, 285 (1972).